nature research

https://doi.org/10.1038/s41929-020-00504-x

Supplementary information

Highly active and stable stepped Cu surface for enhanced electrochemical CO_2 reduction to C_2H_4

In the format provided by the authors and unedited

Supplementary Information for

Highly active and stable stepped Cu surface for enhanced electrochemical CO_2 reduction to C_2H_4.

Chungseok Choi[1], Soonho Kwon[2], Tao Cheng[2,3], Mingjie Xu[4,5,6], Peter Tieu[7], Changsoo Lee[1,8], Jin Cai[1], Hyuck Mo Lee[8], Xiaoqing Pan[4,5,9], Xiangfeng Duan[10], William A. Goddard III[2], and Yu Huang[1*]*

[1]Department of Materials Science and Engineering, University of California, Los Angeles, Los Angeles, California 90095, United States, [2]Department of Applied Physics and Materials Science, California Institute of Technology, Pasadena, California 91125, United States, [3]Institute of Functional Nano & Soft Materials (FUNSOM), Jiangsu Key Laboratory for Carbon-Based Functional Materials & Devices, Joint International Research Laboratory of Carbon-Based Functional Materials and Devices, Soochow University, Suzhou, Jiangsu 215123, People's Republic of China, [4]Irvine Material Research Institute (IMRI) and [5]Department of Materials Science and Engineering, University of California, Irvine, Irvine, California 92697, United States, [6]Fok Ying Tung Research Institute, The Hong Kong University of Science and Technology, Guangzhou 511458, P. R. China, [7]Department of Chemistry, University of California, Irvine, Irvine, California 92697, United States, [8]Department of Materials Science and Engineering, Korea Advanced Institute of Science and Technology, Yuseong-gu, Daejeon, 34141, Republic of Korea, [9]Department of Physics and Astronomy, University of California, Irvine, Irvine, California 92697, United States, [10]Department of Chemistry and Biochemistry, University of California, Los Angeles, Los Angeles, California 90095, United States

*Correspondence to: yhuang@seas.ucla.edu (Y.H.), wag@caltech.edu (W.A.G.)

This PDF file includes:

Supplementary Figures 1 to 15

Supplementary Tables 1 to 6

Supplementary References

Supplementary Figures and Tables

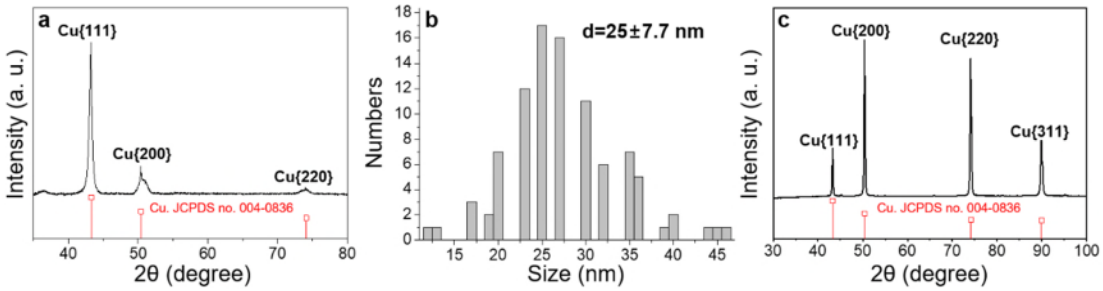

Supplementary Fig. 1 | (**a**) PXRD of Syn-CuNWs, (**b**) Size of Syn-CuNWs. The size was determined by averaging more than 100 NWs. (**c**) PXRD of polycrystalline Cu-foil.

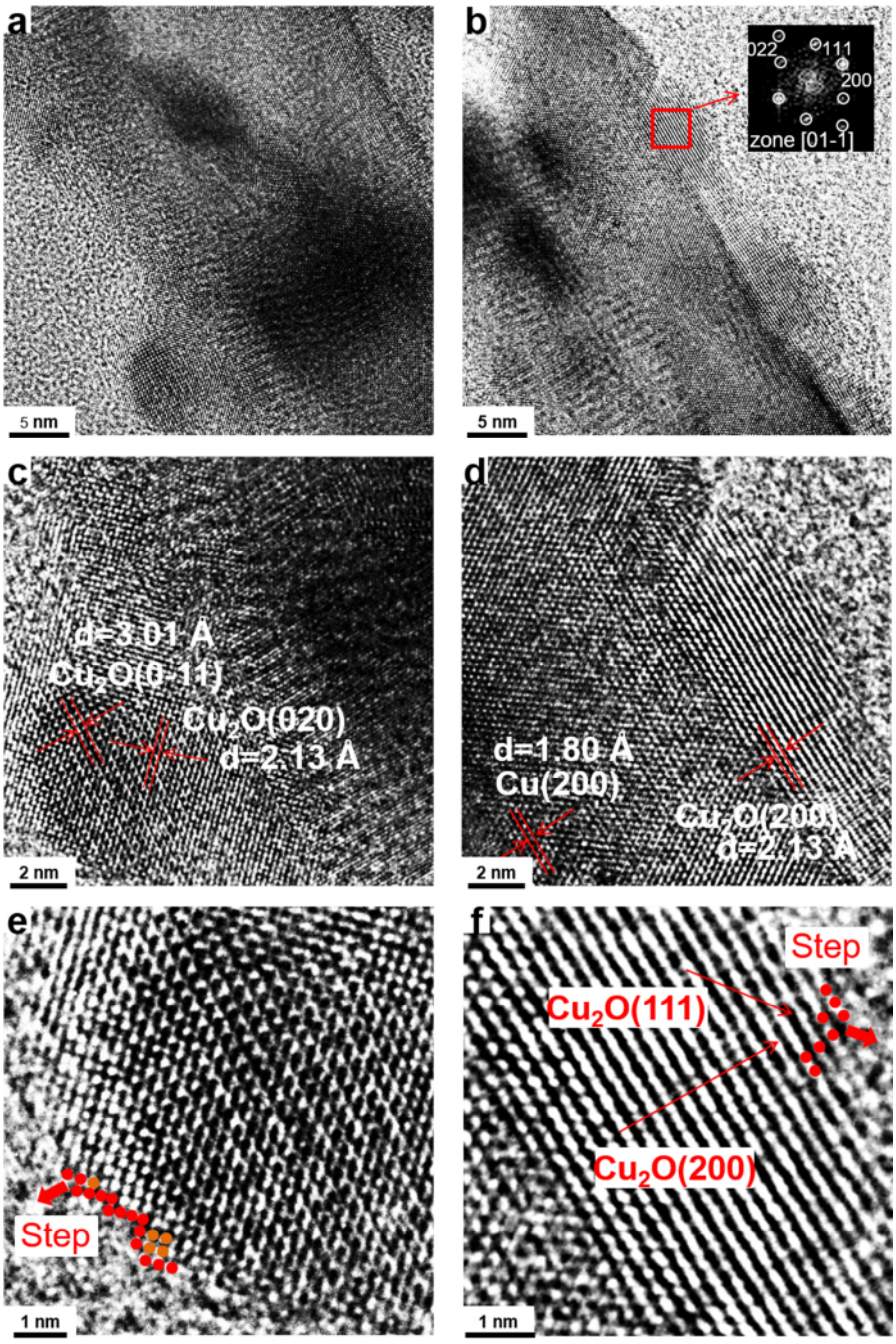

Supplementary Fig. 2 | The highly stepped surface of A-CuNWs after the activation process, (**a**), (**b**) FFT on parts of A-CuNW, (**c**), (**d**) HRTEM images of the surface of A-CuNW, (**e**) [n(001) x (011)] steps on the surface of A-CuNW, (**f**) [n(100) x (111)] on the surface of A-CuNW.

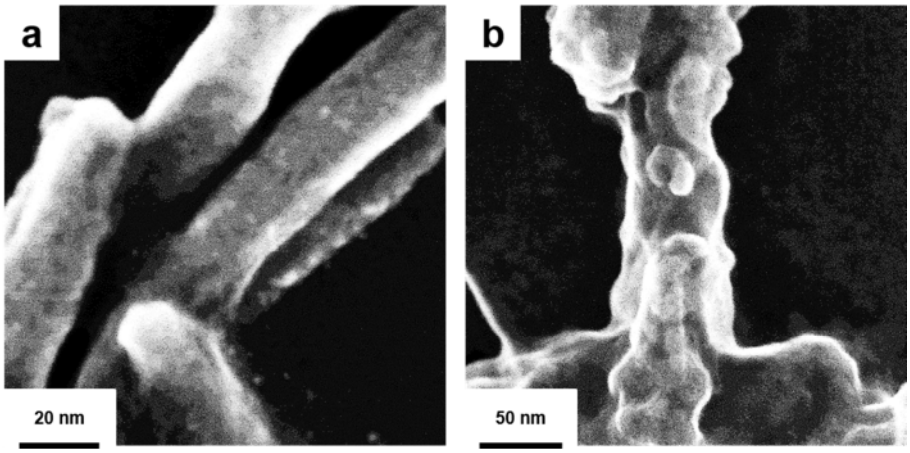

Supplementary Fig. 3 | (**a**) SEI of Syn-CuNWs, (**b**) SEI of A-CuNWs.

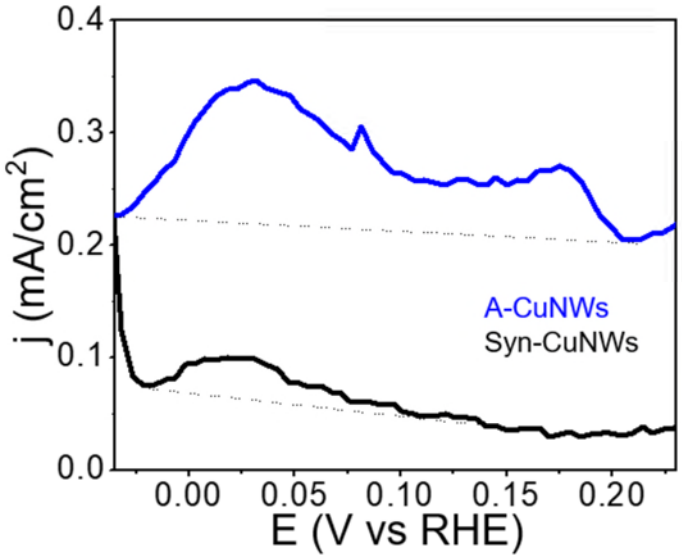

Supplementary Fig. 4 | Pb under-potential deposition (UPD) of Syn-CuNWs (black line) and A-CuNWs (blue line) to extract ECSA measured in N_2-saturated 0.1 M $HClO_4$ + 0.001 M $Pb(ClO_4)_2$ solution at room temperature. The background current (dotted lines) were measured in N_2-saturated 0.1 M $HClO_4$.

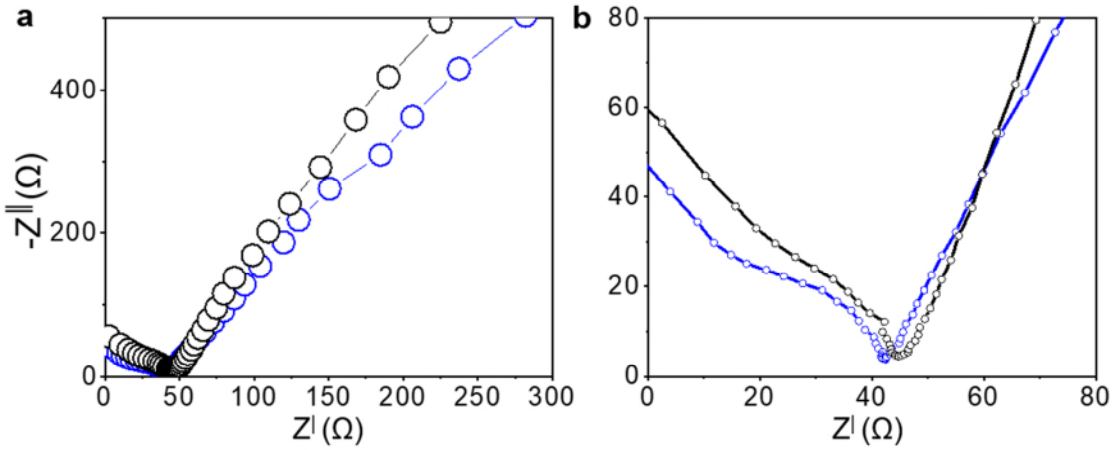

Supplementary Fig. 5 | (**a, b**) Nyquist plot of Syn-CuNWs (black) and A-CuNWs (blue).

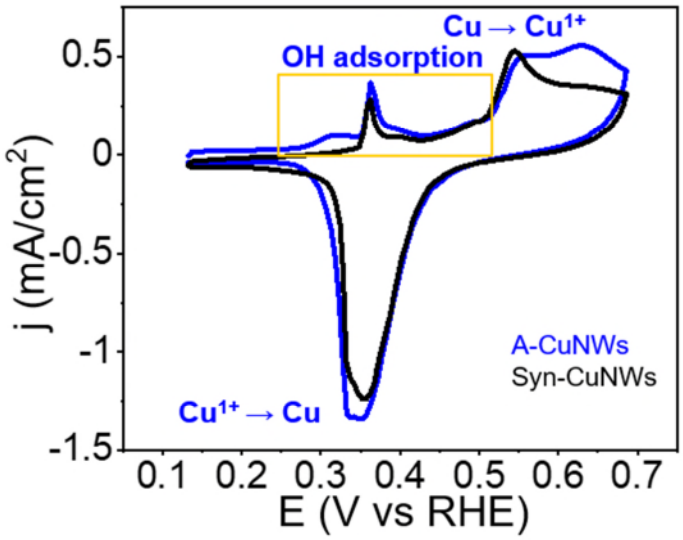

Supplementary Fig. 6 | Redox reaction of Syn-CuNWs and A-CuNWs in 0.1 M KOH at 100 mV/s scan rate. Cu(100) at ~0.362 V[1-4], Cu(110) at 0.395 – 0.43 V[1-4], Cu(111) at ~0.492 V[1-4], and A-(hkl) (high energy steps)[3,4] at a negative shift from Cu(100)).

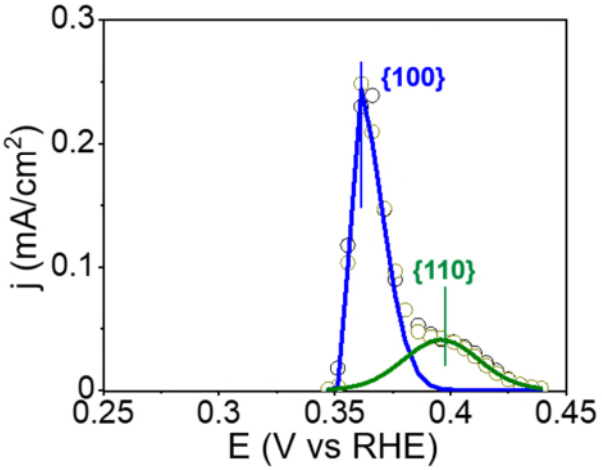

Supplementary Fig. 7 | OH^- adsorption of CuNWs after 10 min of activation. Cu(100) at ~0.362 V (blue color)[1-4], Cu(110) at 0.395 – 0.43 V (green color)[1-4].

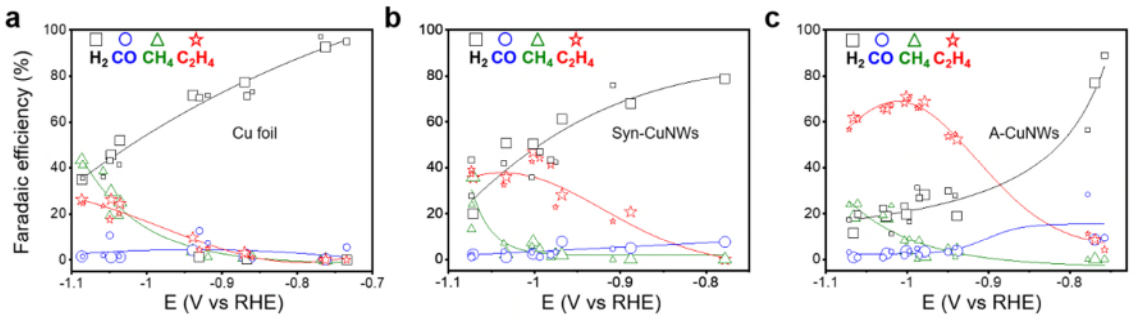

Supplementary Fig. 8 | Electrochemical CO_2RR performance from three independent measurements. (**a**) FEs of Cu foil, (**b**) FEs of Syn-CuNW catalysts, (**c**) FEs of A-CuNW catalysts. Different sizes of the shape indicate different batches of CO_2RR tests.

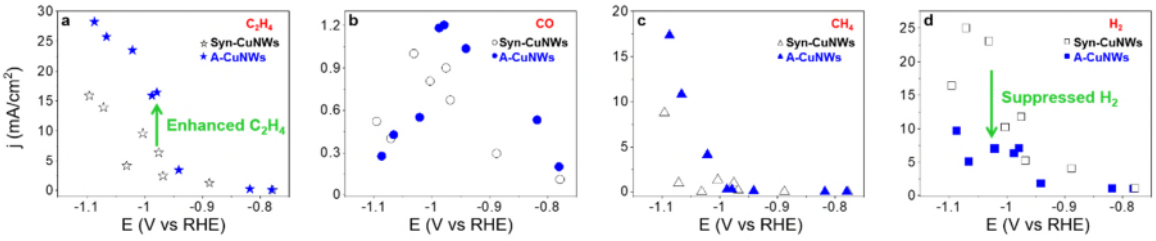

Supplementary Fig. 9 | (**a-d**) Partial current density of Syn-CuNW and A-CuNW catalysts for each product.

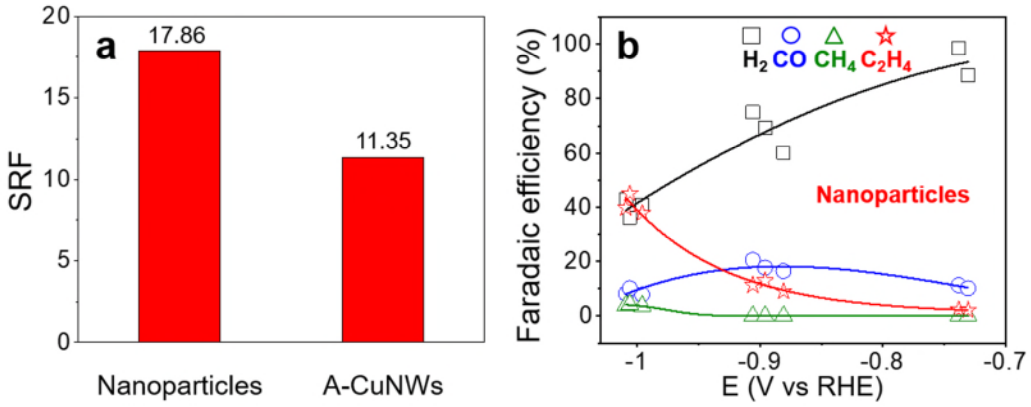

Supplementary Fig. 10 | (**a**) Surface roughness factor (SRF) of commercial-Cu nanoparticles and A-CuNWs, (**b**) FEs for commercial-Cu nanoparticles. The SRF was calculated from CV of electrochemical double-layer from 152 to 202 mV by changing scan rates.

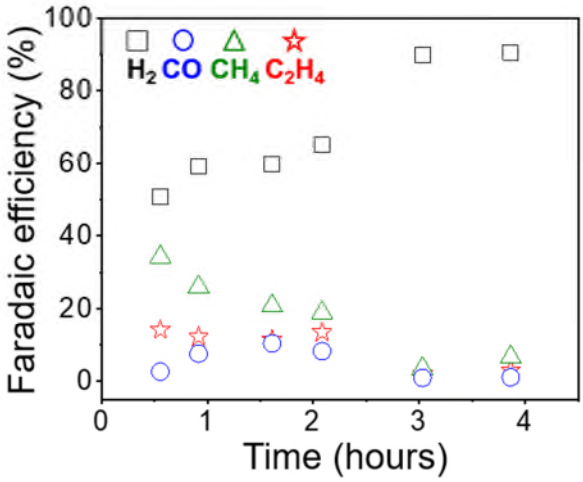

Supplementary Fig. 11 | Stability of Cu foil at -1.07 V in 0.1 M $KCHO_3$.

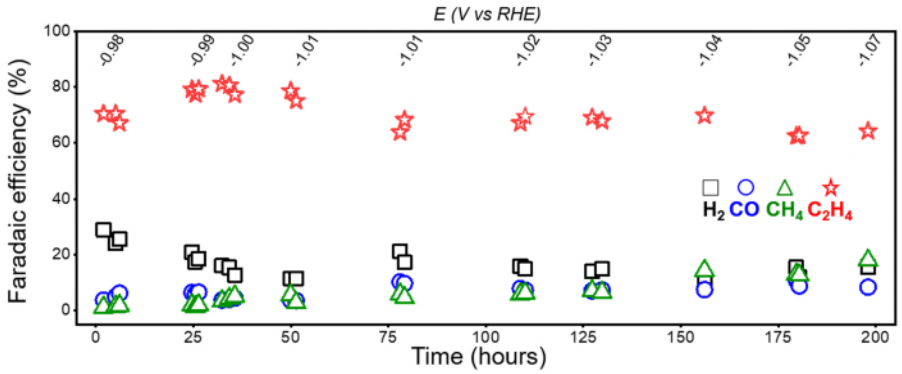

Supplementary Fig. 12 | Stability test of A-CuNW catalysts at potential ranging from -0.98 to -1.07 V (RHE) for 198 hours, Top axis indicates corrected potential.

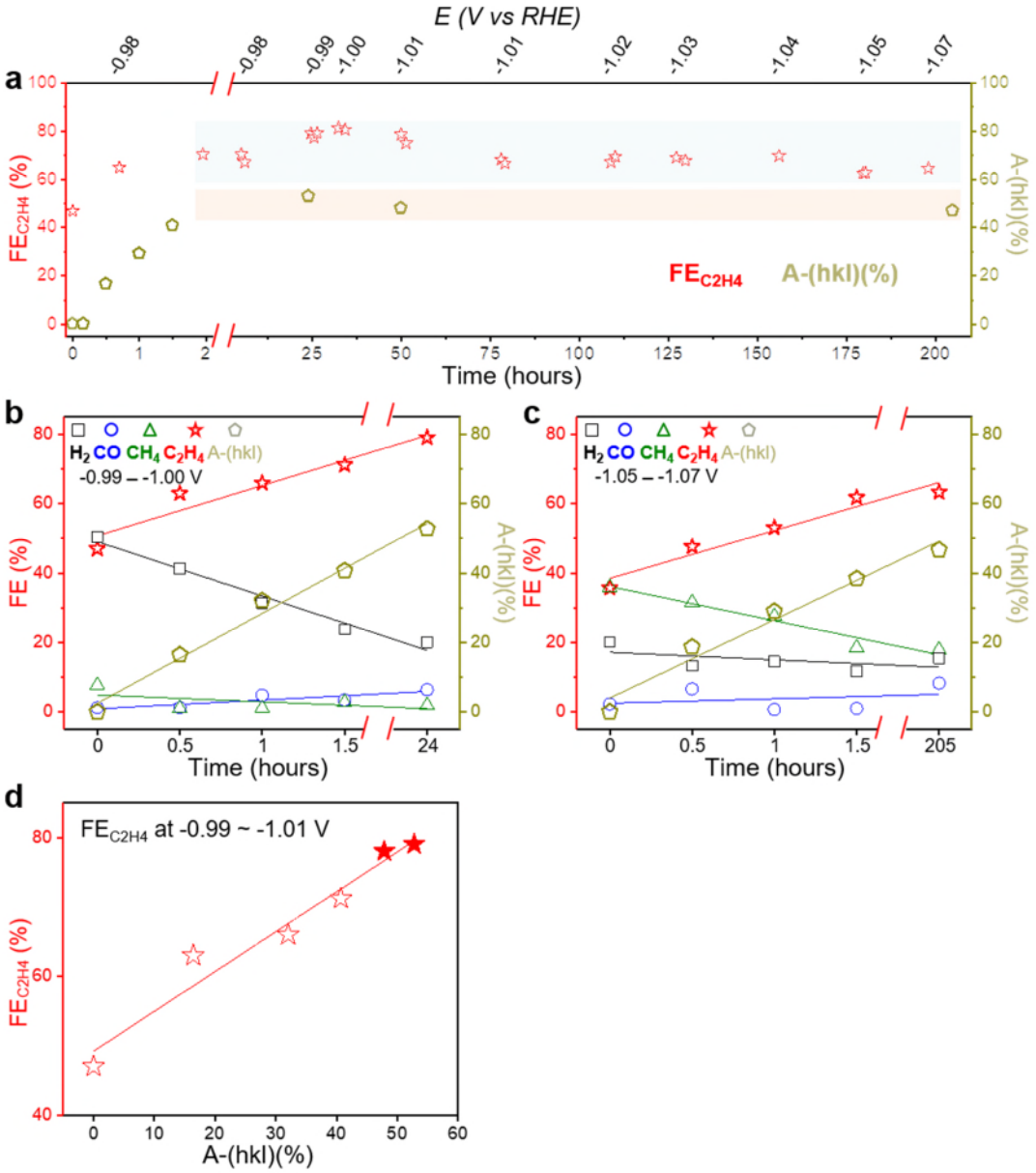

Supplementary Fig. 13 | (**a**) Correlation between A-(hkl) and FE_{C2H4} over the long-term stability test (x-axis is broken at 2.1 h, 0 – 1.5 h correspond to activation period); (**b**) Correlation of both A-(hkl) and FEs with activation times at -0.99 V – -1.00 V (RHE); (**c**) Correlation of both A-(hkl) and FEs with activation times at -1.05 V – -1.07 V (RHE), (**d**) Correlation of A-(hkl) and FE_{C2H4} including data points from stability tests (indicated by solid red stars).

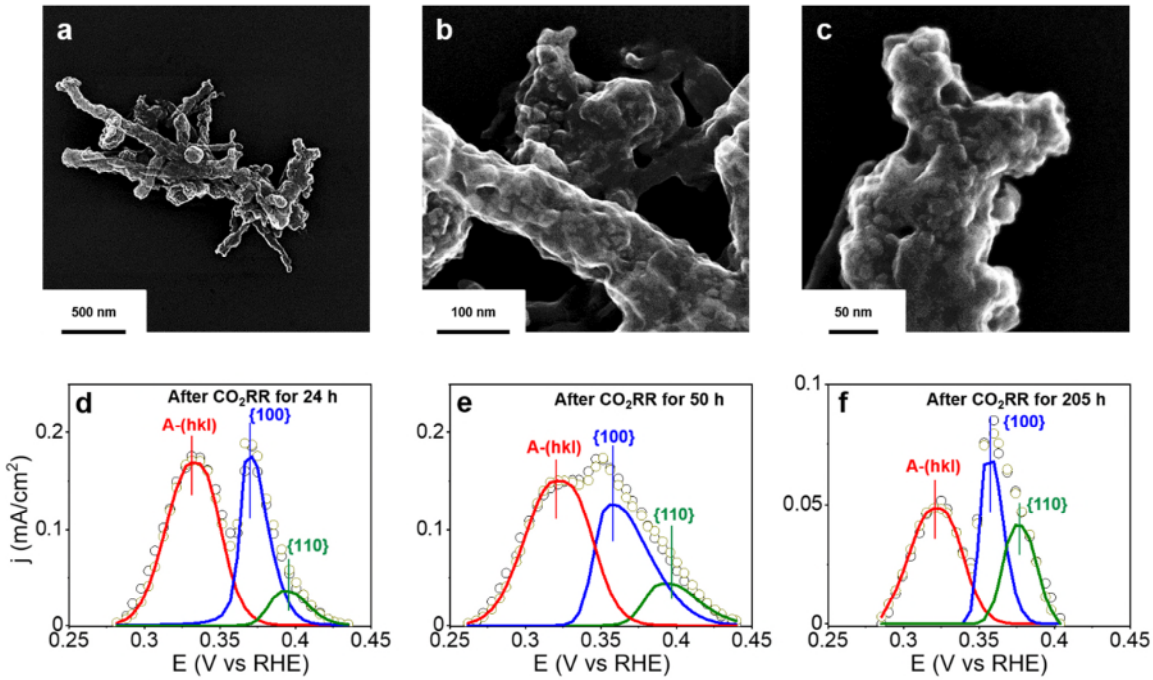

Supplementary Fig. 14 | (**a**) Low magnification SEI of A-CuNW catalysts after CO_2RR for 205 h, (**b**), (**c**) High magnification SEI of A-CuNW catalysts after CO_2RR for 205 h. (**d**) OH^- adsorption of CuNWs after CO_2RR for 24 h, (**b**) after CO_2RR for 50 h, (**c**) after CO_2RR for 205 h. Cu(100) at ~0.362 V (blue color)[1-4], Cu(110) at 0.395 – 0.43 V (green color)[1-4], and A-(hkl) (high energy steps_red colour)[3,4] at a negative shift from Cu(100).

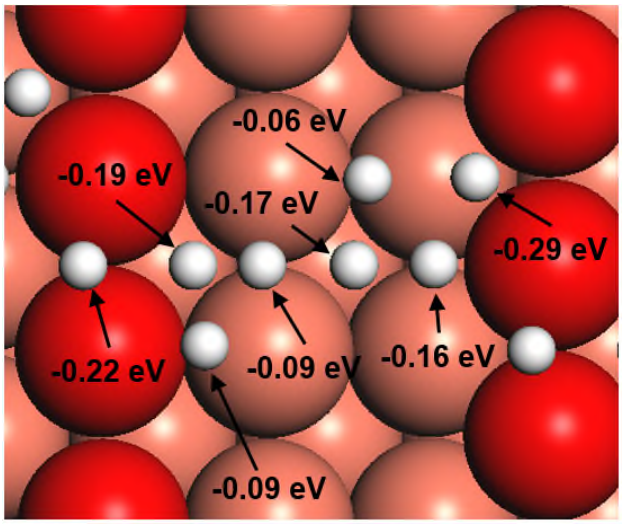

Supplementary Fig. 15 | The H* binding energies of eight possible binding sites on Cu(511). Cu atoms on the step are indicated by red.

Supplementary Table 1 | The surface portions of OH_{ad} on each facet of all catalysts.

Reaction Time	A-(hkl) (%)	Cu{100} (%)	Cu{110} (%)
Before	0	67.49	32.50
10 min	0	73.83	26.16
30 min	17.03	62.38	20.57
1 h	28.98	57.16	13.85
1.5 h	41.12	39.50	19.37
205 h	46.82	31.58	21.58

Supplementary Table 2 | FEs for A-CuNWs. Each point was averaged, and the standard deviation was calculated from three independent measurements.

V (RHE)	H_2%	CO%	CH_4%	C_2H_4%	Ethanol%	Acetate%	Formate%	Total%
-0.76 ±0.01	74.11 ±16.37	15.56 ±11.16	0	8.10 ±3.52	0	0	1.53	99.32 ±4.44
-0.94 ±0.00	25.60 ±5.74	4.05 ±0.98	3.19 ±1.87	53.62 ±1.09	0	0	1.51	87.98 ±6.61
-0.98 ±0.00	28.82 ±2.33	3.35 ±1.47	3.18 ±4.40	67.14 ±1.56	1.50	0	0.73	104.75 ±0.73
-1.00 ±0.00	19.90 ±3.39	3.05 ±1.11	7.09 ±2.71	69.79 ±1.44	2.61	1.35	0.43	104.24 ±1.55
-1.06 ±0.00	16.30 ±4.16	1.65 ±1.28	22.22 ±3.26	59.95 ±2.82	3.39	0	0.24	103.77 ±6.78

Supplementary Table 3 | FEs for Syn-CuNWs. Each point was averaged, and the standard deviation was calculated from three independent measurements.

V (RHE)	H_2%	CO%	CH_4%	C_2H_4%	Total%
-0.89±0.01	63.59±15.01	4.25±0.97	0	22.05±6.02	89.90±9.92
-0.97±0.00	49.02±10.61	4.35±3.06	2.18±1.24	30.76±9.43	86.32±13.64
-1.00±0.00	44.39±7.62	2.23±0.98	6.09±1.49	44.65±2.20	97.38±10.09
-1.03±0.00	51.03±9.74	1.84±1.49	4.29±2.45	34.48±1.75	91.92±7.93
-1.07±0.00	30.44±11.94	1.76±0.69	24.43±11.27	37.25±1.84	93.90±3.00

Supplementary Table 4 | FEs for Cu foil. Each point was averaged, and the standard deviation was calculated from three independent measurements

V (RHE)	H_2%	CO%	CH_4%	C_2H_4%	Ethanol%	Acetate%	Formate%	Total%
-0.75 ±0.01	94.89 ±2.26	2.04 ±2.95	0	0	0	2.08	4.79	103.81 ±3.82
-0.86 ±0.00	73.87 ±3.17	1.51 ±1.40	0.95 ±0.62	2.17 ±1.09	0	1.68	2.91	83.12 ±3.73
-0.93 ±0.00	77.87 ±11.82	6.76 ±5.17	2.42 ±1.22	6.74 ±2.73	0.31	0.46	2.39	96.96 ±8.13
-1.04 ±0.00	46.96 ±4.49	4.36 ±5.59	24.67 ±5.15	22.80 ±4.60	0.91	0.18	0.65	100.53 ±6.71
-1.07 ±0.01	35.59 ±0.62	1.67 ±0.25	40.97 ±2.49	24.81 ±1.38	0.89	0.09	0.22	104.25 ±3.03

Supplementary Table 5 | Summary of stability of C_2H_4 production in H-cell.

Catalysts	Applied potential V (RHE)	Stable FE_{C2H4}	Reported Duration (hours)	Electrolyte	CO_2 Flow rate (sccm)	Source
A-Cu NWs	**-0.97 – -1.07**	**61 – 72%**	**205**	**0.1 M $KHCO_3$**	**15**	**This work**
A-Cu NWs	**-0.98 – -1.07**	**64 – 79%**	**198**	**0.1 M $KHCO_3$**	**15**	**This work**
Cu Nanocube (250 – 300 nm)	- 0.95	45%	1	0.1 M $KHCO_3$	20	(5)
Cu Nanocube (10 – 40 nm)	- 0.75	~32%	10	0.1 M $KHCO_3$	20	(6)
Plasma treated Cu foil	- 0.9	60%	5	0.1 M $KHCO_3$	30	(7)
CuZn nanoparticles	- 1.3	~30%	8	0.1 M $KHCO_3$	20	(8)
Electro-redeposited Cu	- 1.2	40 – 45%	5	0.1 M $KHCO_3$	20	(9)

Supplementary Table 6 | Free energy, frequency, Zero-point energy (ZPE), Enthalpy (Cv), Entropy of all states in DFT calculations.

			Energy [eV]	Frequency [cm^{-1}]	ZPE [eV]	Cv [eV]	TS [eV]
Cu(100)	C1	IS	-263.645	3719.04	1.606498	0.170446	0.232887
		TS	-262.971	3643.092	1.473867	0.179751	0.250323
		FS	-263.98	3716.55	1.731384	0.179365	0.249453
	C2	IS	-263.878	2697.653	0.630043	0.167448	0.253563
		TS	-263.45	2757.024	0.613232	0.13664	0.189569
		FS	-264.291	2751.579	0.674542	0.148478	0.22949
Cu(511)	C1	IS	-207.912	3711.546	1.435686	0.159278	0.221053
		TS	-207.204	3762.022	1.348848	0.189453	0.279913
		FS	-208.391	3759.418	1.583465	0.156297	0.230906
	C2	IS	-208.175	2704.296	0.641028	0.162215	0.24363
		TS	-207.709	2709.244	0.617154	0.140325	0.20639
		FS	-208.316	2813.459	0.680842	0.122072	0.179666

Supplementary References

1. Droog, J. M., & Schlenter, B. Oxygen electrosorption on copper single crystal electrodes in sodium hydroxide solution. *J. Electroanal. Chem.* **112**, 387-390 (1980).
2. Luc, W. *et al.* Two-dimensional copper nanosheets for electrochemical reduction of carbon monoxide to acetate. *Nat. Catal.* **2**, 423-430 (2019).
3. Raciti, D. et al. Low-overpotential electroreduction of carbon monoxide using copper nanowires. *ACS Catal.* **7**, 4467-4472 (2017).
4. Gennero De Chialvo, M. R., Zerbino, J. O., Marchiano, S. L., & Arvia, A. J. Correlation of electrochemical and ellipsometric data in relation to the kinetics and mechanism of Cu_2O electroformation in alkaline solutions. *J. Appl. Electrochem.* **16**, 517-526 (1986).
5. Gao, D. *et al.* Plasma-activated copper nanocube catalysts for efficient carbon dioxide electroreduction to hydrocarbons and alcohols. *ACS nano* **11**, 4825-4831 (2017).
6. Kim, D., Kley, C. S., Li, Y., & Yang, P. Copper nanoparticle ensembles for selective electroreduction of CO2 to C2–C3 products. *PNAS* **114**, 10560-10565 (2017).
7. Mistry, H. *et al.* Highly selective plasma-activated copper catalysts for carbon dioxide reduction to ethylene. *Nat. commun.* **7**, 12123 (2016).
8. Reller, C. *et al.* Selective electroreduction of CO2 toward ethylene on nano dendritic copper catalysts at high current density. *Adv. Energy Mat.* **7**, 1602114 (2017).
9. De Luna, P. *et al.* Catalyst electro-redeposition controls morphology and oxidation state for selective carbon dioxide reduction. *Nat. Catal.* **1**, 103-110, (2018).